Factors Affecting the Hardness Characteristics of Microstructures in Gas Carburized Chromium Alloy Steels

Chang-Yeol Oh[1], Bo-An Kang[*2], Choon Yoo[3], Sang-Jin Yoon[4]

[1]Director/PhD., Professional Qualification Bureau/Management, Human Resources Development Service of Korea(HRDK), Ulsan, Korea
[*2]Professor, Department of Electrical Engineering, Nambu University, Gwangju, Korea
[3]CEO/PhD., Park&Jang Technical Law Firm Vehicle Technology Research Institute, Incheon, Korea
[4]Professor, Department of Mechanical Engineering, Nambu University, Gwangju, Korea
ocy203@naver.com[1], bakang@nambu.ac.kr[*2], fbichoon@naver.com[3], sjyoon@nambu.ac.kr[4]
Corresponding author*: mobile Phone: +82-10-8756-5787

Article History:Received:11 november 2020; Accepted: 27 December 2020; Published online: 05 April 2021

Abstract : We analyzed the factors affecting the gas carburizing microstructure of parts for constant velocity joints. Gas carburizing 0.15-0.20C1.13-1.14Cr chromium alloy steel used in automobile drive units is characterized by changing the properties of the carburizing layer in the depth direction.

The experimental conditions were set to enable field application. The components of the specimen to be used for gas carburization were analyzed by X-ray fluorescence. Changes in the mechanical properties of the carburized layer were analyzed by micro-hardness, microstructure, and carburizing content. The gas carburization cycle was selected based on the simulation results. The characteristics change before and after carburization of two samples with different carbon and chromium content were analyzed.

The carburization temperature that can be used for manufacturing automobile parts was 930°C, the carbon potential required for carburization was 0.90wt%, and the carbon potential required for diffusion was 0.75wt%. The inner and outer hardness values of the carburized layer satisfying the effective hardening depth of 550Hv were 400Hv-740Hv. In the case of 0.20C alloy steel, the effective hardening depth with a carburizing amount of 0.36wt% and a hardness of 550Hv was 1.467 mm. also in the case of 0.15C steel, its effective hardening depth was 0.746 mm. The simulation results for selecting the carburizing heat treatment conditions and the carbon change in the carburizing layer showed a similar trend. The carburizing structure related to hardness change was martensite. As a result of EPMA, SEM, and XRD analysis, the amount of carburized and the amount of martensite structure correlated, and the martensite increased as the amount of carburized increasing. As a result of EPMA analysis, the smaller the carburizing content the greater the depth of carburization.

We intend to proceed with optimization conditions for mass production in connection with wear resistance and fatigue. It is expected that these results will contribute to the improvement of durability of automobile driving parts.

Keywords: Automobile Drive Units, Chromium Alloy Steel, Carburized Layer, Martensite, Hardening depth, Carbon potential.

1. Introduction

Low carbon chromium alloy steel is used as the material in the automobile drive units. Economical carburizing method should be able to massive production in a short time. In order to carburize auto parts in large scale, it is necessary to optimize the processing conditions. Automotive constant velocity joints consist of outer race, inner race, cage and ball. The inner race and cage used as a part of the power transmission device can be easily destroyed, so that the wear resistance and hardness according to the depth of carburization must be high through transformation of the metal structure. Gas carburization is a heat treatment method that is mainly used to improve mechanical properties by improving the impact resistance and increasing the hardness of the surface, thereby providing excellent wear resistance and low internal hardness[1,2]. Gas carburizing has many advantages over solid carburizing and is very suitable for mass production. When carburizing, the temperature is adjusted to 850-950℃ depending on the carburizing depth. In general, to shorten the carburizing time, the carbon potential and carburizing temperature can be increased[1]. Carbon potential refers to the carburizing concentration. If the carbon potential is 0.8%, it means that the carbon concentration can be carburized up to 0.8%. Conversely, when the carbon potential is set to 0.5%, even in the case of 0.8% C steel, decarburization may reduce the carbon of the steel surface to 0.5%. This means that the amount of carburization on the steel surface can be determined according to the carbon potential. If the carbon potential is set too high, soot may occur in the furnace. However, soot can occur in the furnace or damage the structure of the furnace. Occasionally, carbides on the surface of the alloy steel or residual austenite may increase[3,4]. Therefore, in this study, the effects of changes in carburization conditions on the properties of the carburization layer are analyzed from hardness and microstructure.

2. Experimental Methods

[*]**Corresponding author:** Bo-An Kang
Professor, Department of Electrical Engineering, Nambu University, Gwangju, Korea . bakang@nambu.ac.kr

2.1. Chromium alloy steel analysis

Cold-forged chromium alloy steel was used for the carburizing specimen. The chemical composition of the specimen was qualitatively and quantitatively analyzed by unknown elements using X-ray Fluorescence analyzer (Brucker, WD-XRF Tiger). Two types of chromium alloy steel for specimens were used as shown in Table 1.

The inner race (SCR-420H)and cage(SCR-415H) for the constant velocity joint used for carburizing are shown in Figure 1.

Table 1. Chemical composition of chromium alloy steels

Elements	Specimens(wt%)	
	SCR-415H	SCR-420H
C	0.150	0.200
Cr	1.130	1.140
Mn	0.840	0.830
Si	0.240	0.250
P	0.013	0.014
S	0.008	0.007
Ni	0.060	0.060

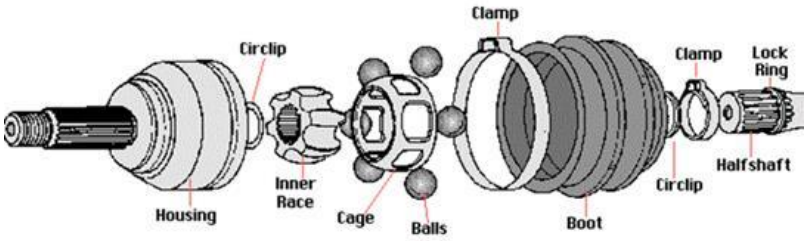

Figure 1. Schematic diagram of the inner race and cage for constant velocity joint

2.2. Gas carburization

In order to use it as an automobile part, the hardness value and carburization depth are required for vehicle life, so the simulated results are reflected in the heat treatment conditions[5]. For the SCR-420H specimen, the carbon potential was maintained 0.9 wt% for 10 hr at 930° C. to infiltrate the surface with carbon. 2.5 liter per minute of propane (C_3H_8) gas was injected into the heat treatment furnace. RX-Gas was maintained at 350m3/hr until carbon diffusion. The carbon potential was kept constant so that the carbon was evenly carburized in the specimen. And for carbon diffusion, a carbon potential of 0.75wt% was maintained for 3hr at 930° C. To prevent specimen deformation and micro-structuring, it was quenched at 840°C for 30 minutes, and then oil cooled at 130°C. For the SCR-415H specimen, The carburization temperature was 930°C, the carbon potential was 0.9wt% and the carburization time was hold 3 hr. Propane gas was injected at 3 ℓ/min, and RX-Gas was maintained at 350 m^3/hr until carbon diffusion. The carbon potential of 0.75 wt% was maintained for 1 hr at a temperature of 930° C. for carbon diffusion on the surface. In the carburizing cycle, the carburizing temperature, carbon diffusion time, carbon potential, and cooling conditions were changed. The carburization cycle curves for the two chromium alloy steels were as shown in Figure 2.

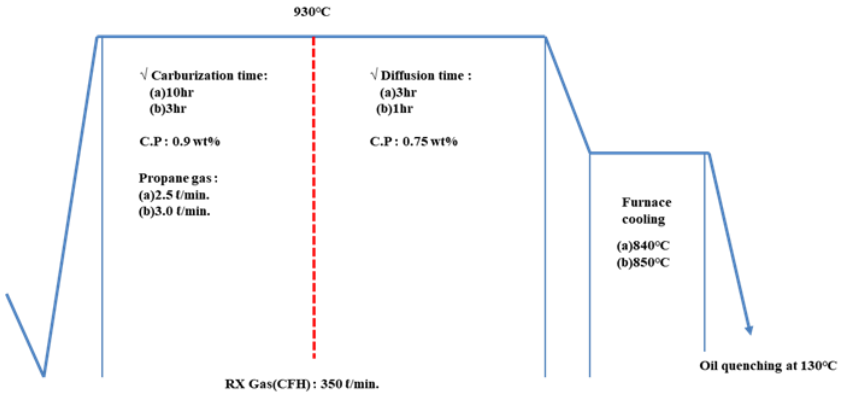

Figure 2. Carburizing cycle for chromium alloy steels: (a)SCR-420H, (b)SCR-415H

2.3. Specimens preparation

To observe the effect of composition and carbon on the microstructure of the carburized specimen, it was collected by cutting vertically from the surface layer in the inner direction. The carburized specimens were cut and mounted to a size of about 10 mm to facilitate polishing. The two specimens were mounted as shown in Figure 3 to measure the carburization amount and observe the microstructure. The polishing was polished by hand using abrasive paper, and in the final step, the surface of the specimen was smoothed at 200 rpm using a 1 μm diamond oil-based paste excellent in polishing with a polishing machine.

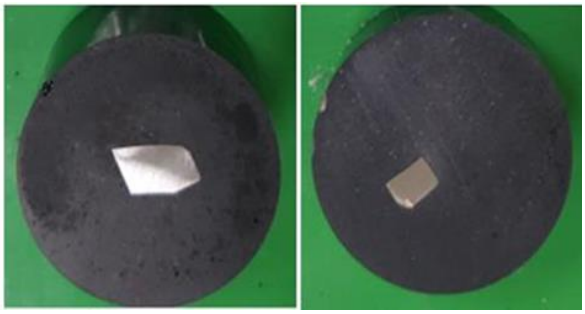

Figure 3. Carburized specimens. (a) SCR-415H, (b) SCR-420H

2.4. Hardness analysis

The microhardness was measured on the mounted specimen as shown in Figure 3. The surface hardness of the two specimens before and after carburization was analyzed using a Rockwell hardness tester. Hardening depth was analyzed by a micro Vickers hardness tester(VLPAK2000). The measurement of the curing depth was kept constant at a load of 300kgf and a load time of 10 sec in the depth direction from the surface. Since the measurement error may occur if the indentation interval is close, the measurement was performed by the zigzag (W) method.

2.5. Microstructure analysis

Nital solution was used as an etchant for microstructure observation and carburized layer analysis. The microstructure observed the surface and deep structures, and observed x 200 and x 500 with an optical microscope (OM, Olympus BX51), and x 2,000, x 5,000 and x 10,000 with a scanning electron microscope (SEM, Hitach S-3000H). The cross-sectional structure of the carburized layer was observed by SEM, and the relationship between carburization depth and hardness, carburization amount and hardness, microstructure transformation was analyzed. The main observations were made to analyze carburization uniformity, surface abnormality layer formation, structure transformation on hardness by carburization depth, grain boundary oxide formation, change in carbon amount and relationship with hardness. Crystal phase analysis before and after carburization was measured in a range of 20 to 80 degrees under CuKα radiation, 40 kV, 300 mA, and 5 deg/min. using a high-power X-ray diffractometer (Bruker corperation, D8 ADVANCE). XRD intensity was indexed using a JCPDS card. To precisely analyze elemental components from the surface of the carburized specimen to the inside[6,7].

EPMA (Electron Probe Micro-Analyzer) was used. The WDS (Wavelength dispersive X-ray spectrometer) spectroscopy system is a system using a single crystal spectroscopy system, and the resolution is determined by the flatness of the specimen and the slit size of the sensing device. The system also uses X-ray wavelength, proportional to the number of electrons focused on the anode, and can measure up to 105 per second. In this study, since the peak width of the X-ray spectrum was narrow, it was analyzed using a WDS method suitable for qualitative and quantitative analysis.

3. Result discussions

The results of simulation with EUROTHERM (S/W, England, Version 2.0) to set the optimal carburizing conditions are shown in Figures 4 and 5. The simulation is a result of assuming an effective curing depth of 550 Hv and a carbon composition of 0.36% at a target carburization depth of 0.5 mm at 900-960°C. The temperature at which a hardening depth that satisfies the automotive parts standard for SCR-420H was suitable at 930°C, the carbon potential of the carburizing section was 0.9 wt%, and the carbon potential of the diffusion section was 0.75 wt%. also in the case of SCR-415H, It was analyzed that the carbon potential in the carburizing section was 0.9 wt.%, and in the diffusion section was 0.75 wt%[8].

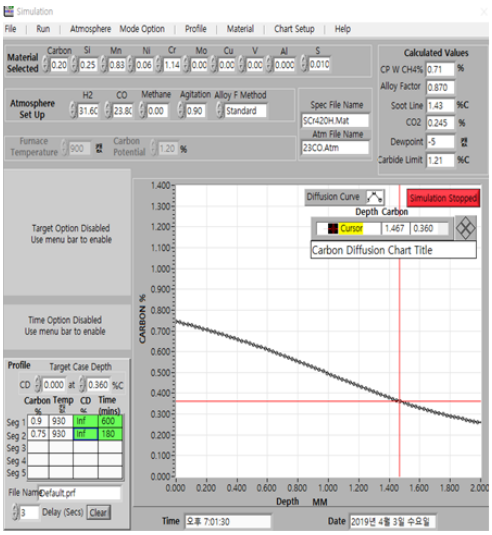

Figure 4. Simulation result at hardening depth 1.467 mm
(Temp. 930 ℃, C/C.P 0.9, D/C.P 0.75, C.T 10hr, D.T 3hr)

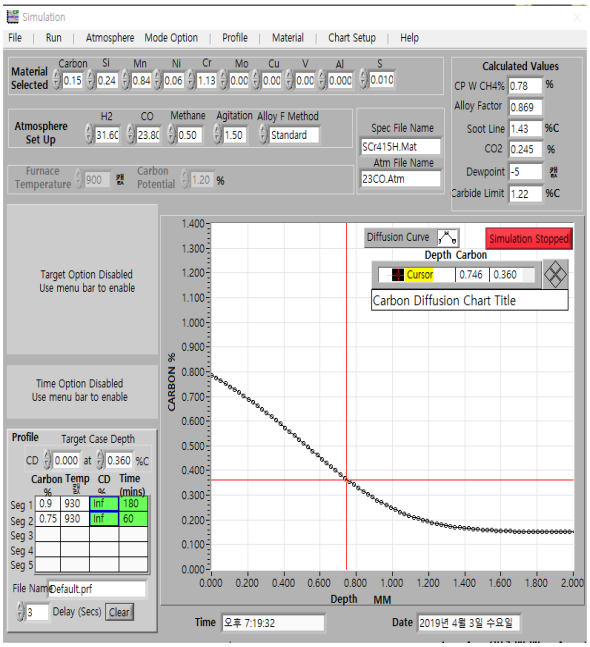

Figure 5. Simulation result at hardening depth 0.746 mm
(Temp. 930 ℃, C/C.P 0.9, D/C.P 0.75, C.T 3hr, D.T 1hr)

Figure 6 is showed the relationship between carburization time, carburization depth, and carburization temperature to obtain hardness values that can be used as constant velocity joint based on simulation results of the SCR-420H and SCR-415H specimens. It was showed that the most suitable carburizing temperature that satisfies the curing depths of 1.467 mm (SCR-420H) and 0.746 mm (SCR-415H) is 930°C. As shown in Table 2, the carburization temperature according to the effective carburization depth of 550Hv, the carburization amount of 0.36% C, and the carburization depth of 1.467mm was 930°C. Carbon potential is 0.9wt in the carburizing section. %, 0.75 wt% in the diffusion section[9].

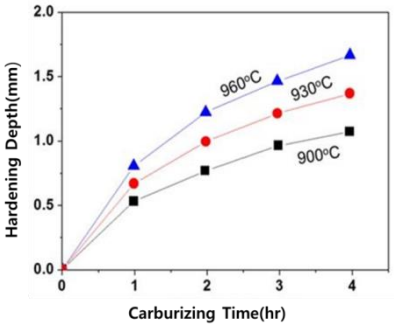

Figure 6. Carburizing temperature suitable for average carburizing time and carburizing depth of chromium alloy steel

As shown in Figure 7, the results of measuring the hardening depth (effective hardening depth 550Hv, 0.36% C), it was showed 0.594-0.734 mm at 900 ℃. It was found to be 0.725-0.877 mm at 930 ℃ and 0.869-0.930 mm at 960 ℃. In the case of the SCR-415H specimen, the hardening depth was 0.746 mm under conditions of an effective hardening depth of 550 Hv and a carburizing amount of 0.36% C required by automobile manufacturers.

As shown in Figures 8 and 9, the change in hardness of the carburized layer is related to the amount of carburization and microstructure. The carburized layer was transformed into a martensite structure due to the penetration of carbon. The hardness of the carburized layer according to the carbon content of the specimen showed a similar trend[10,11].

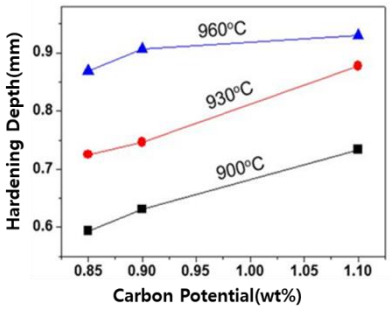

Figure 7. Hardening depth relationship between carburizing temperature and carbon potential(SCR-415H)

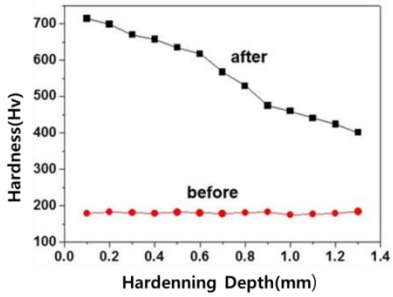

Figure 8. Hardness variation before and after carburization in SCR-415H

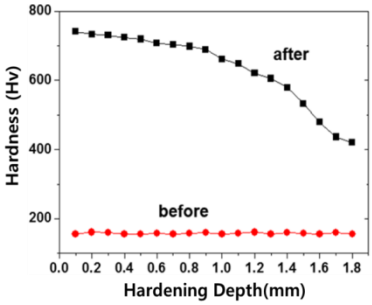

Figure 9. Hardness variation before and after carburization in SCR-420H

The microstructure before carburization was ferrite and pearlite. The presence of metastable cementite in the carburized SCR-415H is thought to be attributable to the Cr alloy element, which is a carbide-forming element.

Table 2 compares the automotive parts standards with the results after carburizing. In the case of SCR-415H, the micro Vickers hardness value at 0.1 mm from the specimen surface was the highest with 714 Hv, and at 401 Hv at 1.3 mm from the surface, it was 43.8% lower. In the case of SCR-420H, the carburizing depth was 0.5 mm more carburized, and the effective curing depth was twice higher than that of SCR-415H 0.7 mm. In both specimens, the degree of carburization and hardness was lowered toward the depth. As a result of carburizing the two specimens, The reason for the difference of hardness between the inside and the surface seems to be related to the carbon penetration and diffusion due to gas carburization. The higher the hardness value, the greater the amount of carburization, and the lower the hardness value, the less the amount of carburization[11].

Table 2. Standards for automotive parts and carburizing results

Specimens	Standards for automotive parts			Carburized layer		
	Carburizing Depth(mm), (Hv513)	Surface Hardness (HRC)	Inside Hardness (HRC)	Carburizing Depth(mm), (Hv513)	Surface Hardness (HRC)	Inside Hardness (HRC)
SCR-420H	1.3-1.7	58-63	25-45	1.54	61	35
SCR-415H	0.7-1.0	58-63	25-45	0.83	60	32

Figure 10 shows that after carburizing the SCR-420H specimen, the surface carbon content increased more rapidly than before carburizing.

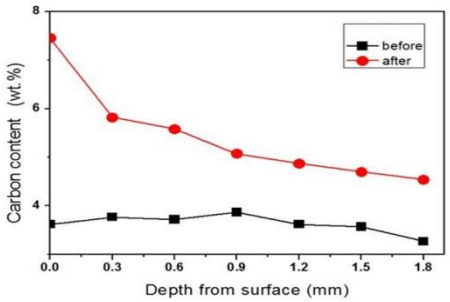

Figure 10. carbon content with carburized depth in SCR-420H before and after carburizing

The carbon content rapidly decreases by 0.3mm on the surface of the carburized sample, and the deeper the depth of carburization, the lower the carbon content. Figure 11 shows the change of carbon content before and after carburizing of the SCR-415H specimen. As a result of comparing the carbon content before and after carburizing for the SCR-415H and SCR-420 specimens, SCR-415H is considered to have a lower carburization after carburizing because the carbon content of the material is 0.3% wt% lower than SCR-420H. These results are also likely to be related to carburization and diffusion maintenance time.

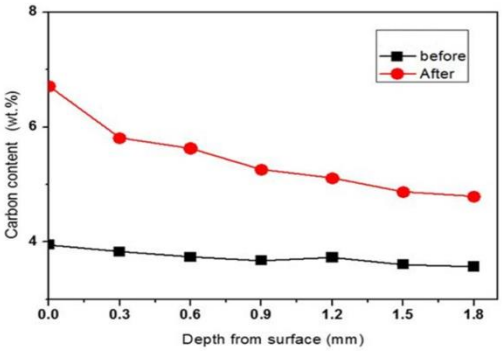

Figure 11. carbon content with carburized depth in SCR-415H before and after carburizing

As shown in Figure 12 and Figure 13, the two carburized specimens were photographed 2,000 times with a scanning electron microscope(SEM) and analyzed with EDS(energy dispersive X-ray spectrometer). The carbon content in the carburized inner layer of SCR-420H was 4.70 wt.%, which was increased by 21% compared to 3.87 wt.% of pre-carburization. As a result of analyzing the scanning electron microscope structure, the raw materials of SCR-420H and SCR-415H before carburization consisted of ferrite and pearlite structures, but were transformed into acicular martensite by carburization. It was confirmed that a residual austenite structure was also present[12].

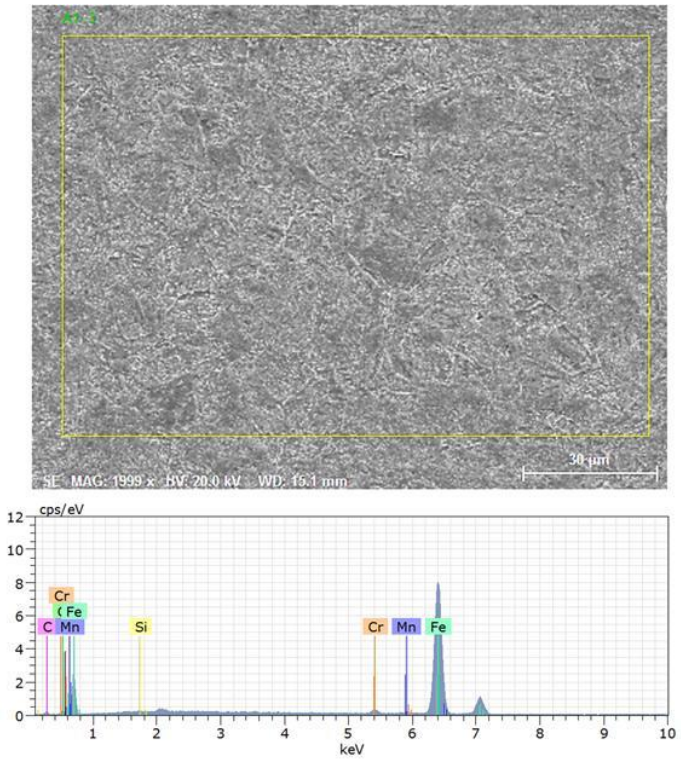

Figure 12. SEM image and EDS spectrum of carburized inner layer in SCR-420H(X2000)

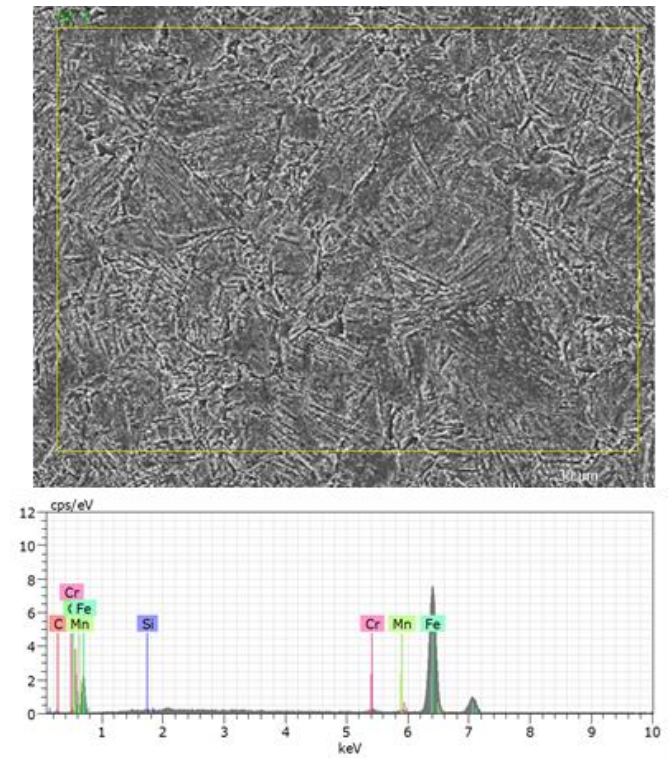

Figure 13. SEM image and EDS spectrum of carburized inner layer in SCR-415H(X2000)

As can be seen in Figures 14 and 15, most of the structure was transformed to martensite after carburizing,

but some residual austenite and ferrite + cementite (Fe_3C) structures remained. Ferrite and pearlite structures were also present. The reason seems to be due to the influence of the alloying elements Mn and Si. The carburized structure showed a BCC structure, and was found to be changed to a martensite structure that contributes to mechanical properties. The BCC crystal structure could be determined by the Miller index, which indicates the direction of the atomic arrangement or the atomic arrangement.

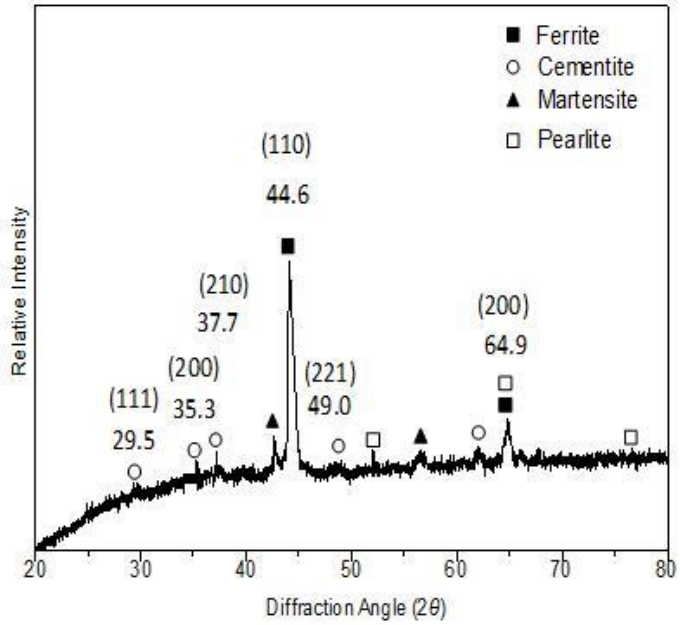

Figure 14. XRD spectrum of carburized SCR-420H

As shown in Fig. 16 and Fig. 17, in the EPMA analysis results, Carbon content gradually decreased from the material surface to the inside. These results tended to coincide with the decrease in hardness values. As a result of the EPMA analysis of SCR-420H and SCR-415H, the carbon content on the surface is higher than the its content in the inner direction of the material, so it seems that carbon penetration was better performed near the surface. In addition, it can be seen that as the carbon diffuses into the material, a concentration gradient occurs and the amount of carbon content gradually decreases[13].

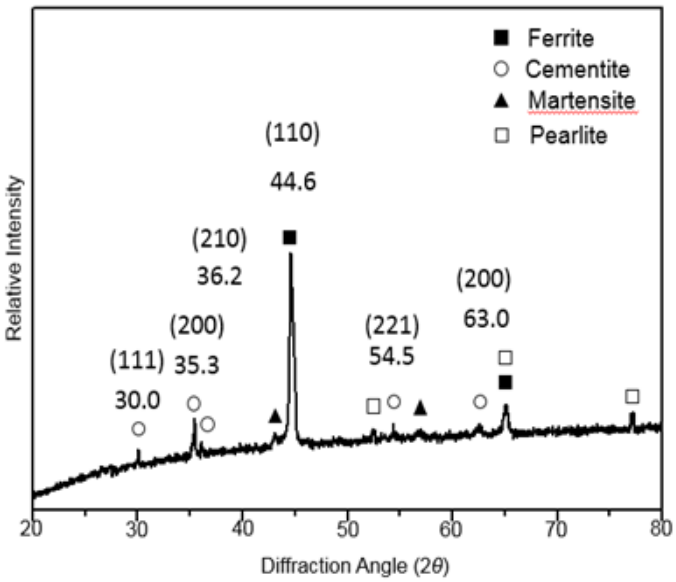

Figure 15. XRD spectrum of carburized SCR-415H

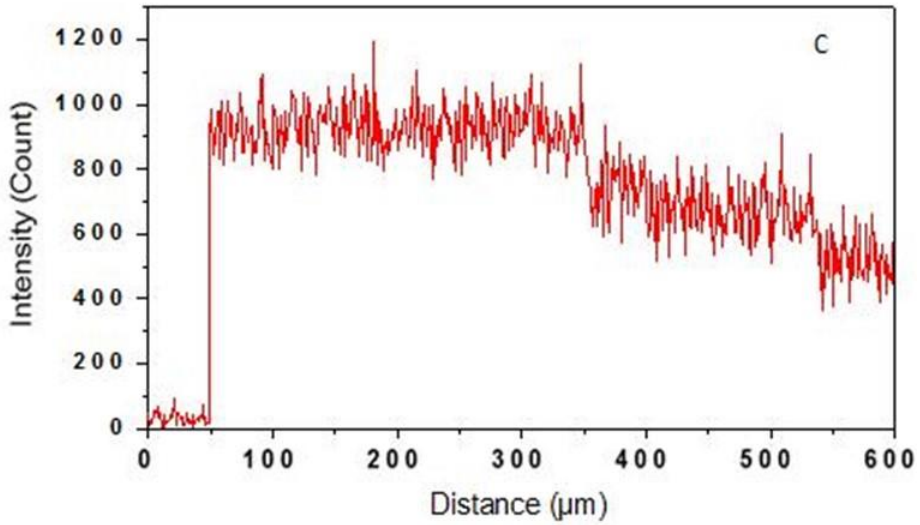

Figure 16. Carbon profile curve of carburized SCR-420H by EPMA

Carbon shows very weak intensity up to 50 μm. High peaks occurred after 50 μm with a large amount of carbon carburization, and the intensity was about 800-1000. In addition, as the peak started to decrease from 350 μm in the first step, it was found that the amount of carburization gradually began to decrease. It was confirmed that the peak decreased as the amount of carburization decreased again near 530 μm. The chromium (Cr) peak occurred at 65-70 μm near the surface containing a large amount of carbon, and the intensity was about 1450[14].

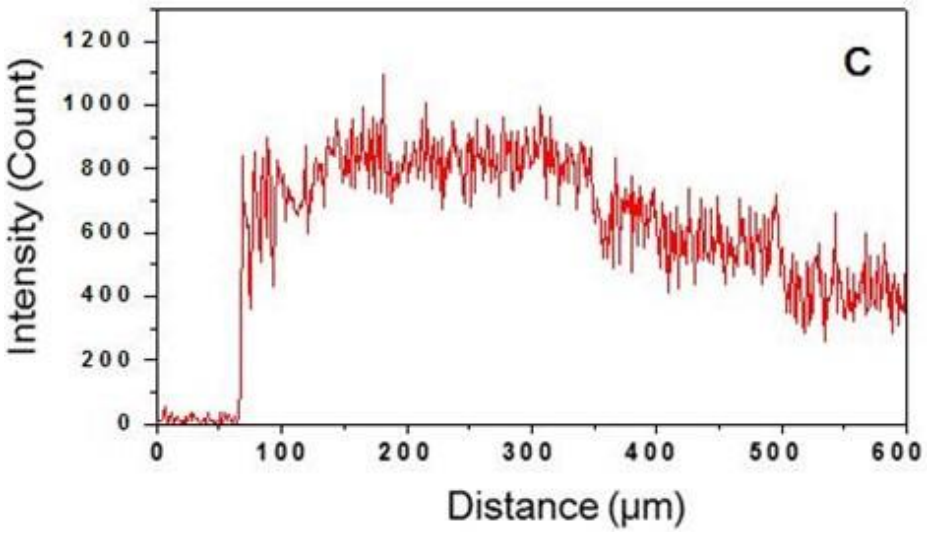

Figure 17. Carbon profile curve of carburized SCR-415H by EPMA

4. Conclusions

In order to mass produce according to the wear resistance standards of automobile constant velocity joints parts by applying laboratory results, it is necessary to determine the optimal conditions through simulation and adjust the parameters during carburization. Especially in mass production, agitation is required to keep the atmosphere constantly in the furnace, and the carburizing temperature and carbon potential must be accurately controlled. The hardness gradient of the carburized layer increased as the carbon content of the material decreased. In order to improve the hardness of the carburized layer, optimization of the conditions of carburization time, diffusion time, and carbon potential and heat treatment after carburization were required. The hardness of the carburized layer was changed according to the degree of the amount of martensite structure. In order to investigate the applicability of the field, we intend to conduct optimization studies on wear resistance and durability.

Acknowledgements

This study was supported by research funds from Nambu University , 2019.

References

Li, Wei, Shuang Deng, and Bingshu Liu. "Experimental study on the influence of different carburized layer depth on gear contact fatigue strength." *Engineering Failure Analysis* 107 (2020): 104225.

Xu, GuangTao, MengFei Hao, YinKui Qiao, YuFang Zhang, Gang Wang, and MingHao Zhao. "Characterization of elastic-plastic properties of surface-modified layers introduced by carburizing." *Mechanics of Materials* 144 (2020): 103364.

Hu, Ke, Guanghong Wang, Xiaoqiang Li, and Shengguan Qu. "Microstructure and formation mechanism in a surface carburized tungsten heavy alloy." *Journal of Alloys and Compounds* 787 (2019): 560-569.

Xiao, Na, Weijun Hui, Yongjian Zhang, Xiaoli Zhao, Ying Chen, and Han Dong. "High cycle fatigue behavior of a low carbon alloy steel: The influence of vacuum carburizing treatment." *Engineering Failure Analysis* 109 (2020): 104215.

Yang, Yang, Kai Zhou, and Guojie Li. "Surface gradient microstructural characteristics and evolution mechanism of 2195 aluminum lithium alloy induced by laser shock peening." *Optics & Laser Technology* 109 (2019): 1-7.

Peng, Yawei, Zhe Liu, Chaoming Chen, Jianming Gong, and Marcel AJ Somers. "Effect of low-temperature surface hardening by carburization on the fatigue behavior of AISI 316L austenitic stainless steel." *Materials Science and Engineering*: A 769 (2020): 138524.

Maharjan, Niroj, Wei Zhou, Yu Zhou, Yingchun Guan, and Naien Wu. "Comparative study of laser surface hardening of 50CrMo4 steel using continuous-wave laser and pulsed lasers with ms, ns, ps and fs pulse duration." *Surface and Coatings Technology* 366 (2019): 311-320.

Anusha, E., Adepu Kumar, and S. M. Shariff. "A novel method of laser surface hardening treatment inducing different thermal processing condition for Thin-sectioned 100Cr6 steel." *Optics & Laser Technology* 125 (2020): 106061.

Moradi, Mahmoud, Hossein Arabi, and Alexander FH Kaplan. "An experimental investigation of the effects of diode laser surface hardening of AISI 410 stainless steel and comparison with furnace hardening heat treatment." *Journal of the Brazilian Society of Mechanical Sciences and Engineering* 41, no. 10 (2019): 434.

Grigoriev, Sergey, Alexander Metel, Marina Volosova, Yury Melnik, Htet A. Ney, and Enver Mustafaev. "Surface Hardening of Massive Steel Products in the Low-pressure Glow Discharge Plasma." *Technologies* 7, no. 3 (2019): 62.

Abhishek, Amber Kumar Dwivedi Chandan Chopra, and Naman Kumar Gandhi Singh. "INVESTIGATION ON SURFACE HARDENING OF MILD STEEL BY CARBURIZING DIFFUSION PROCESS." *Journal Current Science* 20, no. 1 (2019).

Yin, Longcheng, Xinxin Ma, Guangze Tang, Zhongyuan Fu, Shuxin Yang, Tingjian Wang, Liqin Wang, and Liuhe Li. "Characterization of carburized 14Cr14Co13Mo4 stainless steel by low pressure carburizing." *Surface and Coatings Technology* 358 (2019): 654-660.

Hiremath, Pavan, Sathyashankara Sharma, M. C. Gowrishankar, Manjunath Shettar, and B. M. Gurumurthy. "Effect of post carburizing treatments on residual stress distribution in plain carbon and alloy steels–a numerical analysis." *Journal of Materials Research and Technology* 9, no. 4 (2020): 8439-8450.

Wołowiec-Korecka, Emilia, Maciej Korecki, Michał Sut, Agnieszka Brewka, and Piotr Kula. "Calculation of the Mixture Flow in a Low-Pressure Carburizing Process." *Metals* 9, no. 4 (2019): 439.